

The Geomagnetic Effects of Two-dimensional Conductivity Inhomogeneities at Different Depths

F. Walter Jones and Albert T. Price*

(Received 1970 October 22)

Summary

Field distributions and surface effects of two-dimensional conductivity inhomogeneities are investigated. Inhomogeneities of different thicknesses at the Earth's surface and also inhomogeneities of fixed sizes but at various depths are considered. A numerical method is used to solve the differential equations and boundary conditions for the two-dimensional models. The surface variations of the various components are compared for the different dimensions and overburden depths. Important differences are found in the behaviour of the apparent resistivities calculated for H and E polarizations of the applied field.

1. Introduction

In order to construct models of sub-surface conductivity distributions from surface magnetic and electric measurements it is essential to know what each type of structure contributes to the surface effects. When knowledge of the physical effects and the contribution of each parameter are obtained from elementary models, model building of more complex structures will be more effective. Also, it is important to know what effect overburden of different depths has on the surface measurements.

A simple two-dimensional rectangular conductivity inhomogeneity model has been employed to investigate the sub-surface field distributions and the values of the various field components along the surface produced by such inhomogeneities, when an alternating current flows in the conductor, this current being parallel to the surface at great distances from the inhomogeneities.

In previous work, Jones & Price (1969, 1970, 1971) have applied the Gauss–Seidel iteration technique to solve the appropriate equations and boundary conditions for various cases in which a vertical contact between regions of different conductivities exists. This same method has been extended in the present work to consider two-dimensional structures completely surrounded by regions of different conductivity. The results only are given in this paper. The detailed calculations are similar to those described in the paper (1970) quoted above.

2. Description of the models

A semi-infinite conductor occupying the region $z > 0$ with a rectangular region of one conductivity surrounded by a region of different conductivity is taken as the basic model. In the first case (Model 1) the rectangular region lies at the surface of

* Present address: 23 Butlers Court Road, Beaconsfield, Bucks., England

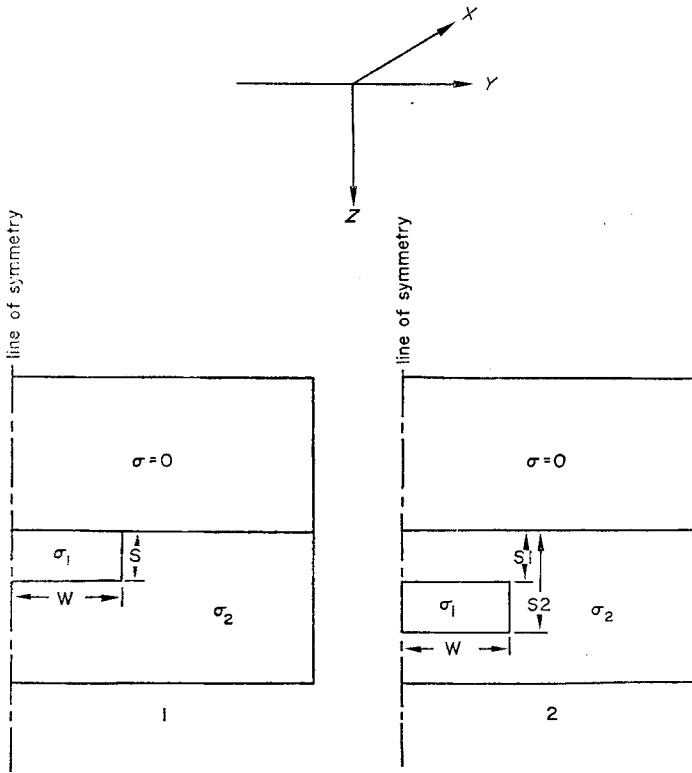


FIG. 1. The co-ordinate system and the two models.

the semi-infinite conductor, and its size is varied by changing the vertical thickness of the inhomogeneous region. This will generally be referred to as the 'surface' anomaly. In the second case (Model 2), the rectangular region lies under the surface and remains constant in size, but the depth of the region from the surface is varied. This will be referred to as the 'sub-surface' anomaly. The two models are illustrated in Fig. 1. The models are symmetric as indicated by the plane of symmetry, and so in every case the solution is obtained for one-half the total region. *

The co-ordinate system used is also shown in Fig. 1. For the two-dimensional problem all quantities are independent of x . For both models the H -polarization case (H parallel to the strike), and the E -polarization case (E parallel to the strike) have been solved. In the H -polarization case H_x is constant along the surface (Jones & Price 1970), but E_y is determined there. In the E -polarization case E_x , H_y and H_z are determined along the surface. Also, the phases of the components and various ratios of interest as well as the apparent resistivity along the surface over the inhomogeneities are determined. For both models the cases $\sigma_1 > \sigma_2$ and $\sigma_1 < \sigma_2$ are considered, for the values of σ_1 and σ_2 shown in Table 1.

The frequency used in this work is 1 Hz, and the conductivities of the various regions as well as the skin depths in the regions at this frequency are given in Table 1. The various depths of the conductivity discontinuities s , s_1 , s_2 (see Fig. 1), for which calculations are made are given in Table 2. In all cases the total width ($2W$) of the inhomogeneous region is taken as 39 km, so that the half-width W used in the calculation is 19.5 km, which covers 13 grid spaces (1.5 km grid distance). The

Table 1*Skin depths in the conductors at $1H_z$*

		Skin depth
$\sigma_1 > \sigma_2$:	$\sigma_1 = 10^{-12}$ emu	1.592 km.
	$\sigma_2 = 10^{-14}$ emu	15.92 km.
$\sigma_1 < \sigma_2$:	$\sigma_1 = 10^{-16}$ emu	159.2 km.
	$\sigma_2 = 10^{-14}$ emu	15.92 km.

Table 2*Dimension and designations of inhomogeneities (See Fig. 1)*

Model 1		Designation	
S		$\sigma_1 > \sigma_2$	$\sigma_1 < \sigma_2$
3 km		A	D
9		B	E
15		C	F
Model 2			
S_1	S_2	$\sigma_1 > \sigma_2$	$\sigma_1 < \sigma_2$
3 km	12 km	A	D
9	18	B	E
15	24	C	F

grid size of the half of the symmetric model is 41×41 (1681 points), and so a cross section 60 km high by 120 km wide is represented. The Earth's surface is taken as the horizontal line of grid points through the centre of the grid.

The various dimensions of the anomalies for which calculations are made for the two models are shown in Table 2. The different cases are designated by letters ABCDEF as shown. To reduce the necessity of cross references, a simplified key is attached to Figs 6 and 8.

3. Field distributions within the conductors

It is assumed that as $y \rightarrow \infty$ or $-\infty$ the alternating field behaves like that for a uniform conductor, so that the distribution of currents and field follows the usual skin effect formula.

The field distributions near the inhomogeneities for the two polarization cases were then determined in detail but the conductivities given in Table 1 lead to rapidly changing fields difficult to exhibit graphically. Hence Figs 2 and 3 show the contours of equal magnitude of E_x (the E -polarization case) for four epochs at equidistant intervals of time during half of one oscillation for a different case in which $\sigma_1 = 10\sigma_2$. This was chosen since it illustrates the distributions better, but the general effects are the same as in the case $\sigma_1 = 100\sigma_2$. The E_x contours are the lines of force of the magnetic field. Figs 4 and 5 show the same four epochs for a case when $\sigma_1 = 0.1\sigma_2$.

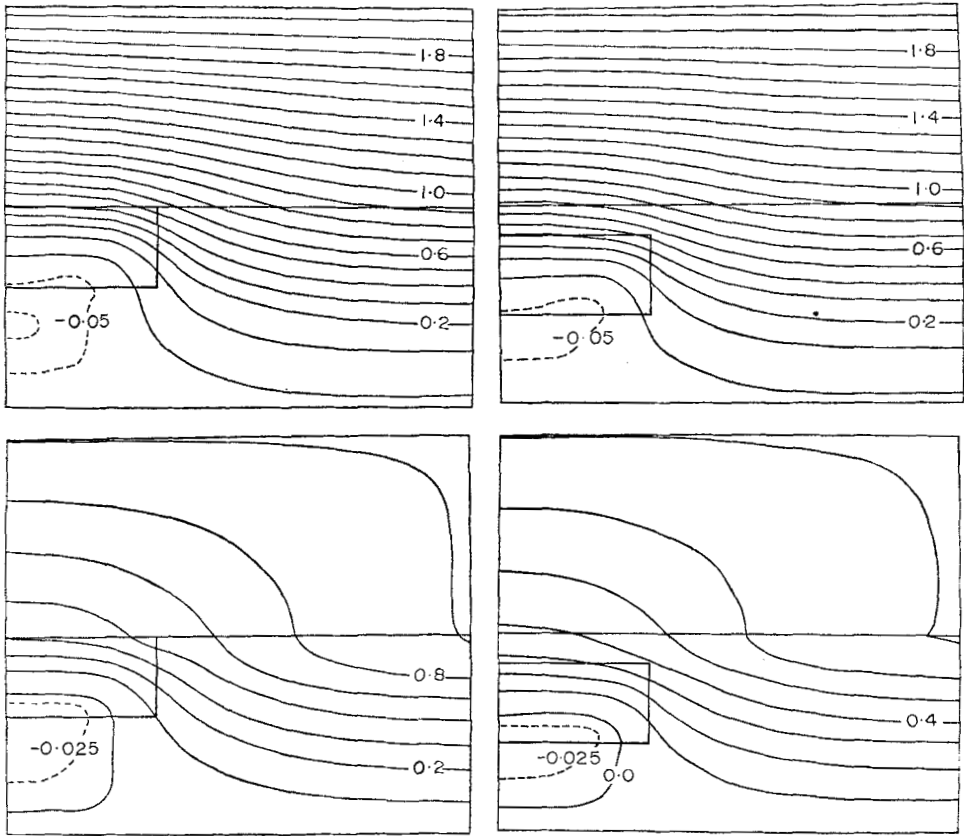


FIG. 2. E -polarization, $\sigma_1 > \sigma_2$, lines of force of H -field (\approx contours of equal E_x) for equal time steps for the two models.

The top diagrams of Fig. 2 show that the electric field is decreasing with depth in the conductor, and the magnetic field lines become further apart corresponding to the skin effect. Beneath the inhomogeneity is a region of negative current around which the magnetic field lines are closed. In the lower pair of diagrams of Fig. 2 the field and current flow at great distances become small, being theoretically zero at infinity, and the existing field is purely the perturbation field at that instant. The top pair of diagrams of Fig. 3 shows that a wedge of high current density has formed in the corner of the higher conducting region of Model 1, whereas a similar wedge of current does not form until later in the model with the higher conductivity region below the surface. It is seen that the region of negative current becomes smaller and the current density decreases as time goes on and eventually disappears. In the lower diagrams of Fig. 3, the wedge has formed in the sub-surface anomaly. As time goes on the positive current wedge moves down through the conductor and decreases in magnitude. The next current wedge formed one-half cycle later will be in the negative sense and will move downward and decrease in magnitude while another positive wedge forms and so on. The current wedge always forms later in the buried inhomogeneity than in the surface inhomogeneity.

Figs 4 and 5 illustrate the same time steps as Figs 2 and 3, but now the rectangular region is of lower conductivity than the surrounding region ($\sigma_1 < \sigma_2$). Again current concentrations are formed in the higher conductivity regions and move downward

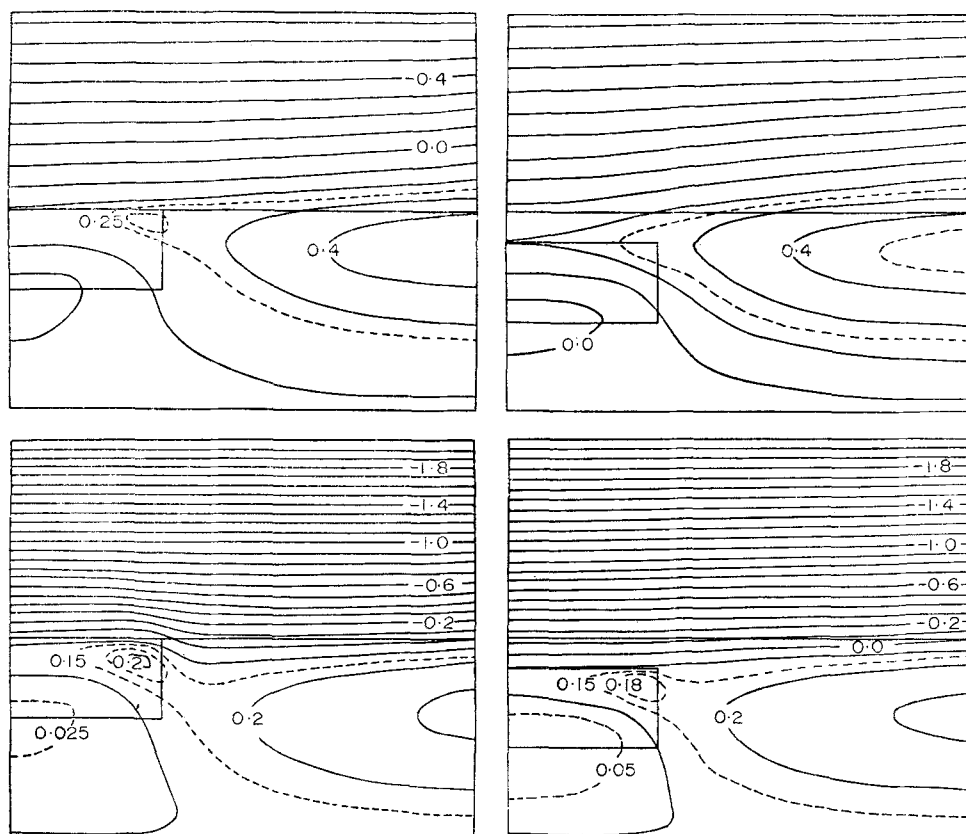


FIG. 3. As Fig. 2, for two further time steps.

through these regions. The lower diagrams of Fig. 4 show the instantaneous perturbation field when the field at infinity is zero for these cases. It is observed that the magnetic field lines are closed to one side of the inhomogeneity in the case of the surface inhomogeneity, and above the inhomogeneity in the sub-surface case. In each case the current concentrations are always formed in the higher conducting regions of the conductors and move downward through these regions.

For the H -polarization cases, current vortices are formed in the corners of the higher conducting regions and move downward through these regions in a similar manner (Jones & Price 1970).

4. Surface effects

(a) H -polarization

For the H -polarization case the surface values of the amplitude of E_y are calculated. Since H_x is constant along the surface this also gives the ratio E_y/H_x . The phase of the y -component of the electric field (ϕ_{E_y}) is computed, as well as the apparent resistivity (ρ_A) for this case. The phase (ϕ_{E_z}) is computed relative to the end surface point, since at every instant the difference in phase between this point and any other point is the same. It should be noted that E_z is zero along the surface of the conductor in both the H -polarization and E -polarization cases (Jones & Price 1970).

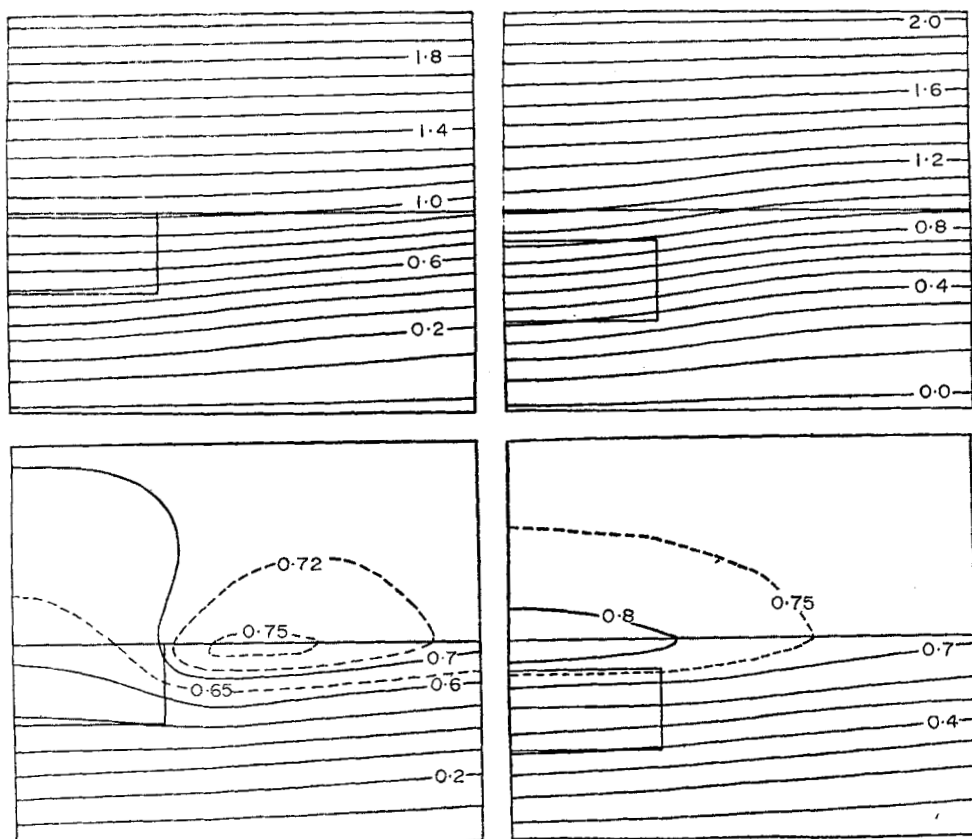


FIG. 4. As Fig. 2, but with $\sigma_1 < \sigma_2$.

Fig. 6 shows ϕ_{E_y} , E_y and ρ_A along the surface for H -polarization for the various thicknesses of the conductor σ_1 in Model 1, and various depths of the conductor in Model 2.

The phase of the horizontal component of the electric field changes along the surface over the inhomogeneity, the changes being quite sudden at the edge of the surface anomaly. For the case $\sigma_1 > \sigma_2$ (A, B, C), as the conductor σ_1 increases in thickness the phase difference between any point and the end surface point appears to approach a constant (negative) value across the top of the anomaly, and there is evidence of a less rapid change in phase at a distance from the anomaly until the actual contact is approached. For the case $\sigma_1 < \sigma_2$ (D, E, F), the relative phase over the anomaly is positive and increases as the anomalous conductor becomes thicker. Also the rate of phase change increases as the anomaly is approached.

For the sub-surface anomaly (Model 2), the case $\sigma_1 > \sigma_2$ (A, B, C) shows that the phase of E_y over the anomaly is positive relative to the phase at a distance from the anomaly. This is opposite to the case where the anomalous conductor is in contact with the surface. It is apparent that the presence of overburden considerably affects the relative phase of this component across the anomaly. Also, it is evident that the overburden has modified the rather abrupt phase changes of the surface anomaly, and they have become much smoother functions over the buried anomaly. It is also seen that as the higher conducting region is buried deeper, the phase changes become less. For the $\sigma_1 < \sigma_2$ case, again the phase change is reversed relative to

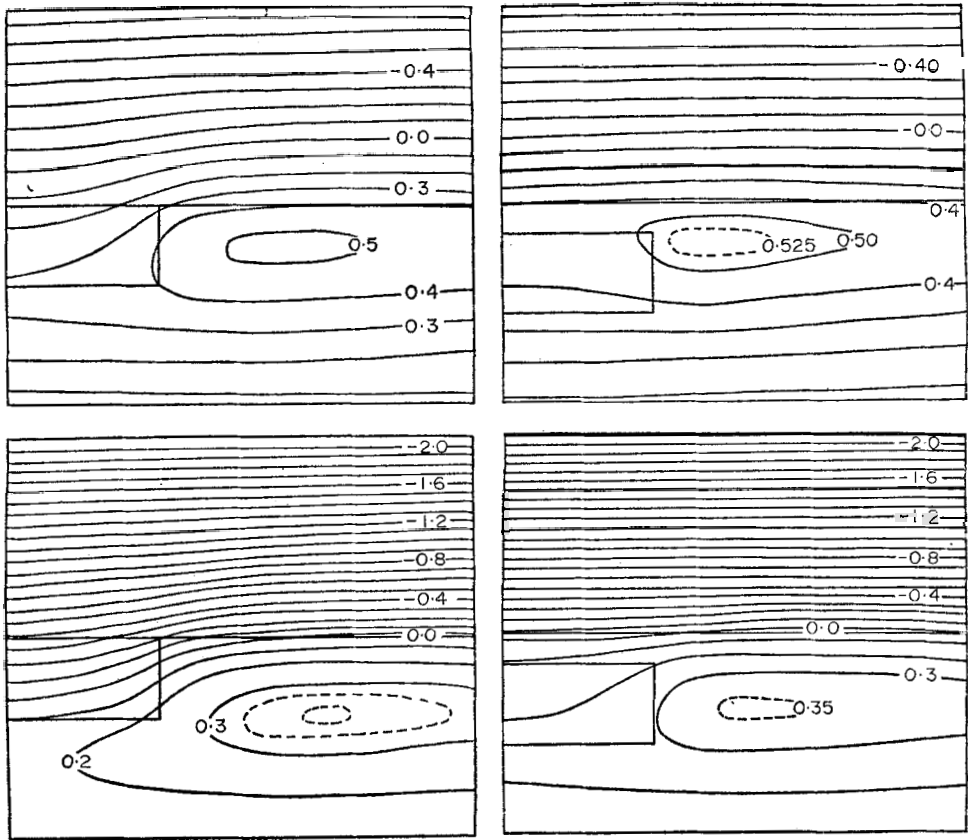


FIG. 5. As Fig. 3, but with $\sigma_1 < \sigma_2$.

the surface anomaly. Also, the phase changes are smooth, but apparently the phase changes do not decrease steadily as the anomaly is placed further from the surface. There may be some critical position at which the effect is a maximum. This may result from the fact that the current vortex always forms in the higher conducting region, and there is a critical size for this region above the lower conductivity region in order that a substantial vortex may be created there. In fact, the current vortex appears to be 'squeezed out' of this region as its dimension becomes small.

The surface values of the amplitude of the horizontal electric field (E_y) are shown for the two models in the centre pair of diagrams of Fig. 6. For the surface anomaly E_y is discontinuous along the surface, and is related to the strong refraction of the lines of current flow at the discontinuity (Jones & Price 1970). Across the boundary between the two conductors the normal component of current is continuous, but since $\sigma_1 \neq \sigma_2$, then E_y is discontinuous. This is an effect of the accumulation of surface charge on the boundary between the two media, and is discussed further in Section 5. For the sub-surface anomaly the horizontal electric field component is continuous. The variations of this component for the various dimensional changes can be seen from the figure. For the surface anomaly and $\sigma_1 > \sigma_2$, E_y approaches a limit over the anomaly and at the contact as its depth dimension increases. For $\sigma_1 < \sigma_2$, the change over the anomaly becomes greater as the thickness of the conductor σ_1 increases. Also, E_y changes more rapidly with distance from the anomaly on the higher conducting side of the anomaly. As the sub-surface anomaly is placed at greater depths the variation of E_y along the surface remains continuous and decreases.

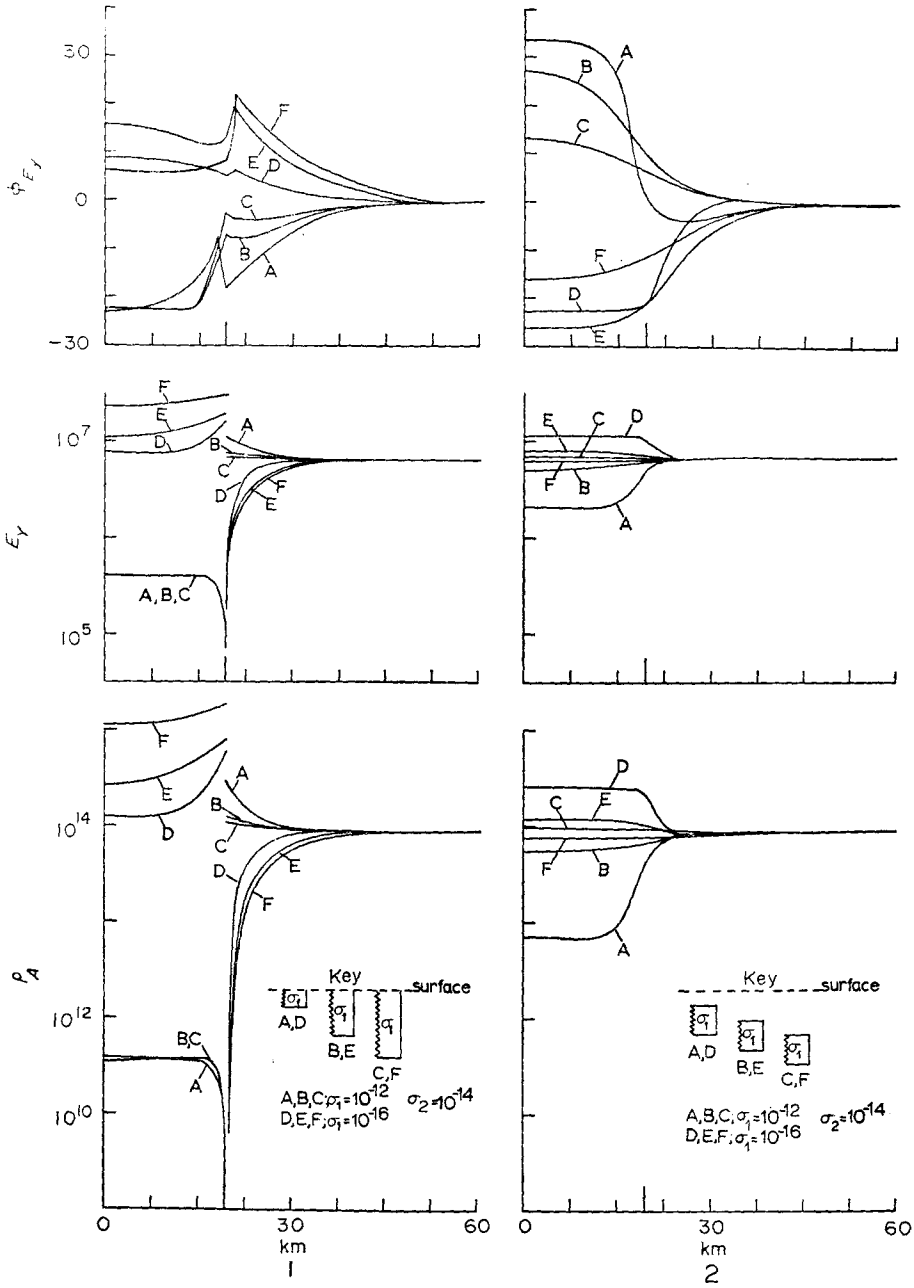


FIG. 6. *H*-polarization, models 1 and 2, surface values of ϕ_{E_y} (degrees), E_y (e.m.u.) and ρ_A (e.m.u. (Ohm-m $\times 10^{11}$)) for the various depths as in Table 2.

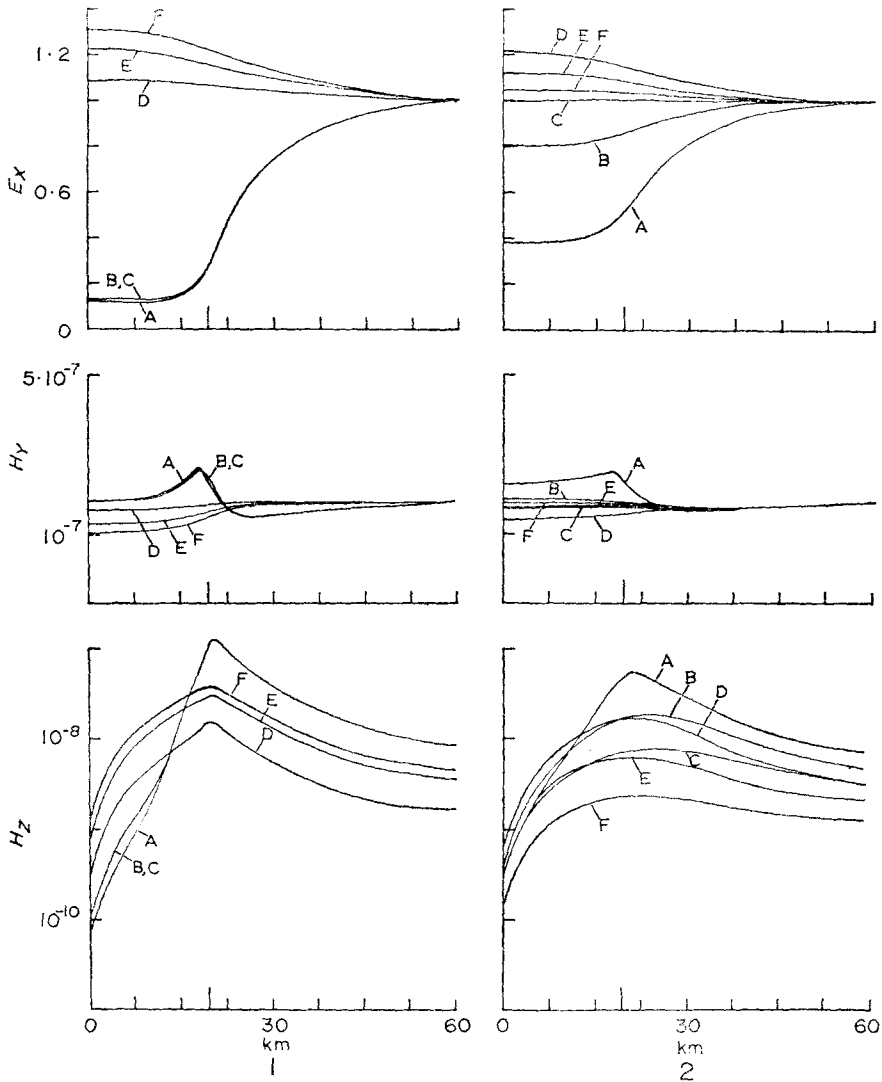


FIG. 7. E -polarization, models 1 and 2, surface values of E_x (e.m.u.), H_y ($\times 10^5$ gammas) and H_z ($\times 10^5$ gammas).

The apparent resistivity across the surface is discontinuous for the surface anomaly, but continuous when there is overburden. The effects on ρ_A for the various parameter changes are similar to the effects on E_y (or E_y/H_x) and are discussed further in Section 5.

(b) E -polarization

For the E -polarization case the surface values of the amplitudes of E_x , H_y and H_z are computed, as well as the ratios E_x/H_y , H_z/H_y and the apparent resistivity ρ_A . The phases of $E_x(\phi_{E_x})$, $H_y(\phi_{H_y})$ and $H_z(\phi_{H_z})$ are also determined along the surface over the anomalies. ϕ_{E_x} , ϕ_{H_y} and ϕ_{H_z} are again calculated relative to the end surface point.

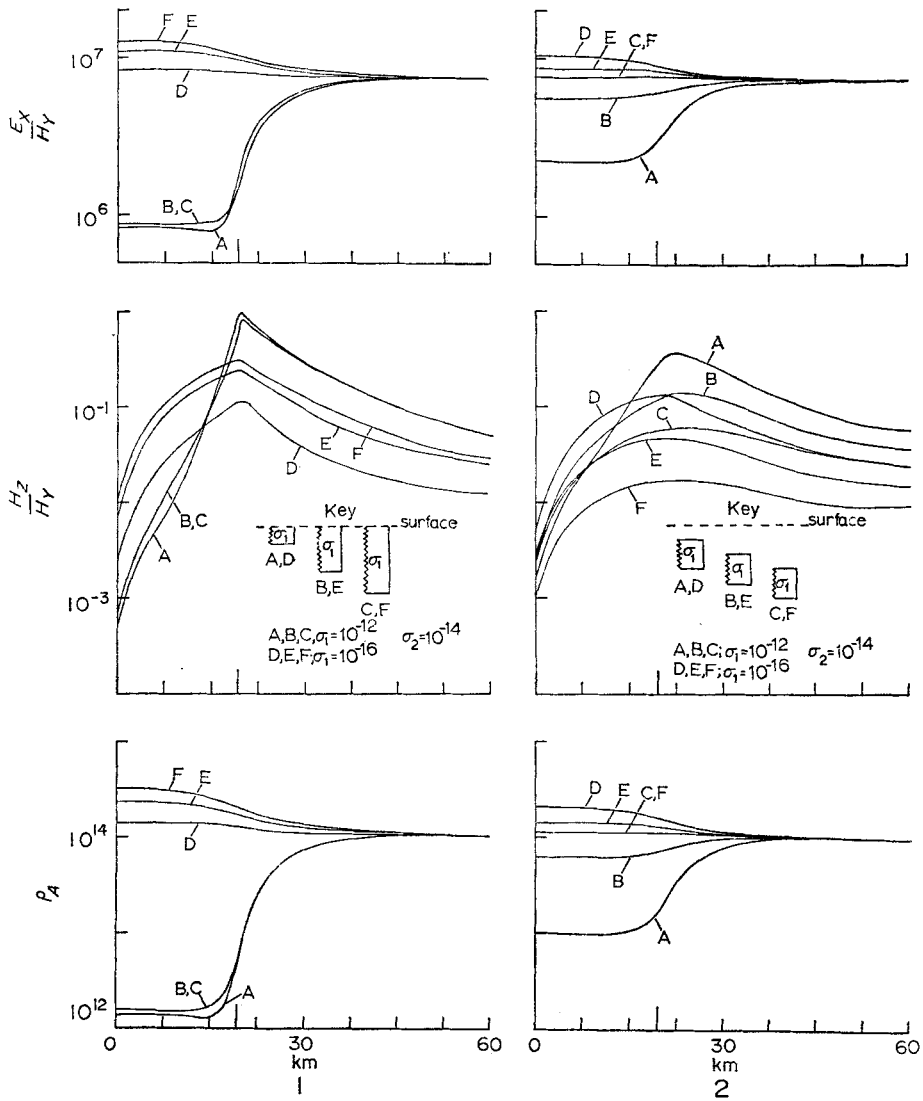


FIG. 8. *E*-polarization, surface values of E_x/H_y , H_z/H_y and ρ_A (e.m.u. (Ohm m $\times 10^{11}$)).

In Fig. 7, E_x , H_y and H_z are plotted for the various dimensions as in Table 2 for the two models. For the surface anomaly when $\sigma_1 > \sigma_2$ (Model 1, A, B, C), there is evidence that the thickness of the anomalous conductor within the limits used here is not critical for the surface effects. When the conductor is below the surface (Model 2, A, B, C), its depth has considerable influence on E_x , since as the depth of burial increases the effect noticeably decreases.

The dimensions of the surface anomaly when $\sigma_1 < \sigma_2$ (Model 1, D, E, F) do have an effect on E_x . As the conductor producing the anomaly increases in thickness, the variation of E_x along the surface becomes greater. Also, for $\sigma_1 < \sigma_2$, the variation of E_x over the sub-surface anomaly (Model 2, D, E, F) decreases as the anomaly is moved to deeper positions.

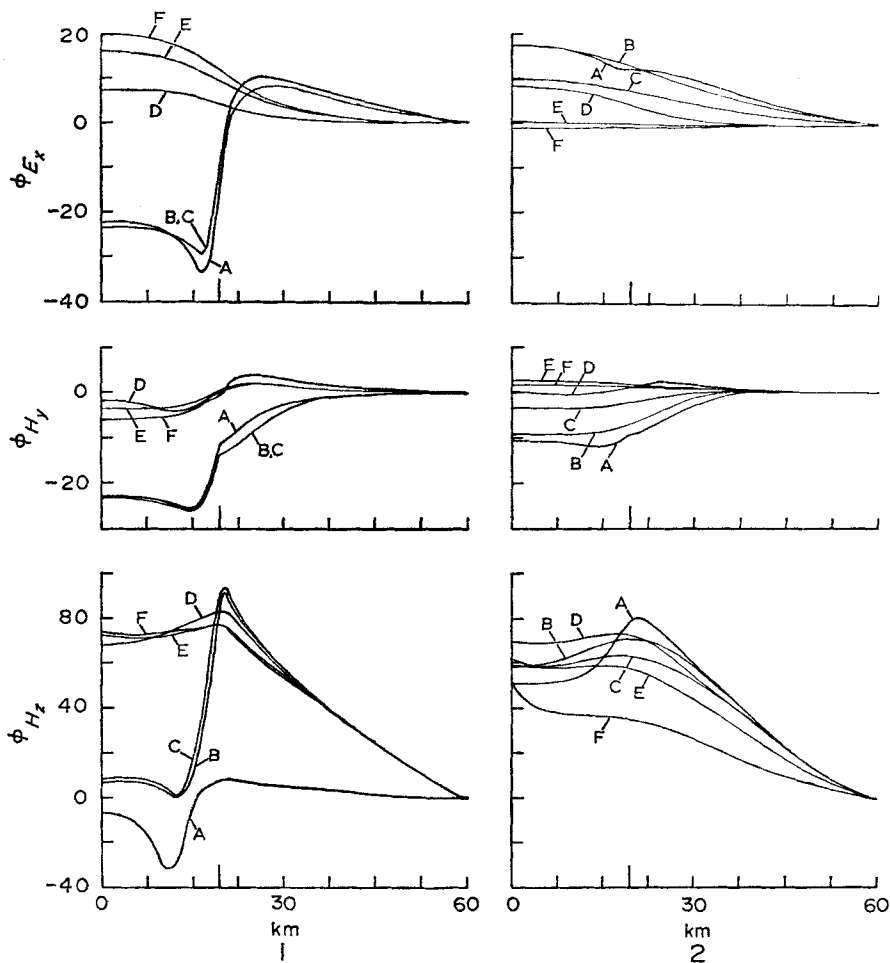


FIG. 9. E -polarization, surface values of ϕ_{E_x} , ϕ_{H_y} , and ϕ_{H_z} in degrees.

From Fig. 7 it is seen that the variation in amplitude of H_y over the anomaly is relatively small compared with that of H_z , although the magnitude of H_y is greater than that of H_z . In the case $\sigma_1 > \sigma_2$ the surface anomaly gives a 'bump' in H_y over the discontinuity. This 'bump' occurs over the sub-surface discontinuity as well and becomes less prominent as the depth of overburden is increased. For $\sigma_1 < \sigma_2$ there is a smoother change in H_y across the surface. The variation increases for the surface anomaly as the conductor thickness increases; for the sub-surface anomaly the variation decreases as its depth increases and eventually becomes negligible.

Fig. 7 shows that the variation of the amplitude of H_z across the surface is greater than the variation of the amplitude of H_y . This is different from the result where the surface values of H_z and H_y were calculated across the surface over a contact between two semi-infinite quarter-spaces of different conductivity (Jones & Price 1970), but the difference is probably due to the fact that in that calculation the conductivity ratio was 10, whereas in the present work the conductivity ratio is 100 (see also Jones & Price 1971). Again, the variation of H_z with depth and dimensions of the

conductivity slab is shown in the figure. For $\sigma_1 > \sigma_2$ the surface anomaly dimensions affect H_z only slightly, while for $\sigma_1 < \sigma_2$ the effect is to increase the variation in H_z as the low conductivity slab becomes thicker. For the sub-surface anomaly the variation of H_z becomes less pronounced for both $\sigma_1 > \sigma_2$ and $\sigma_1 < \sigma_2$ as the anomaly is placed at greater depths.

Fig. 8 gives the ratios E_x/H_y , H_z/H_y and ρ_A for the E -polarization. These ratios indicate similar effects as do the components themselves, and the effects of dimensional and depth changes are evident.

The phase variations of $E_x(\phi_{E_x})$, $H_y(\phi_{H_y})$ and $H_z(\phi_{H_z})$ are shown in Fig. 9. For $\sigma_1 > \sigma_2$, ϕ_{E_x} for the surface anomaly changes phase over the anomaly in the opposite sense, relative to the end point, to the phase change over the buried inhomogeneity. The phase change over the anomaly which is of lower conductivity than its surroundings is in the same sense for both the surface and buried anomalies. The variations with dimensions and depths are shown in the figure, which also shows the phase changes of H_y and H_z . The influence of the overburden is particularly evident in ϕ_{H_z} . The greatest difference between the surface and buried anomalies occurs when $\sigma_1 > \sigma_2$. It is apparent that the effect of overburden is to greatly reduce the drop in the phase difference in H_z on crossing over the edge of the anomaly. A curious feature of the results for the surface anomaly is the remarkable difference between the curve A and the curves B and C. It is difficult to account for this, but it may be associated with the fact that the skin depth for σ_1 is slightly greater than half the thickness of the conductor A, while for B and C it is a much smaller (and probably negligible) fraction of the thickness.

5. Conclusions

The behaviour of the surface field over an anomaly is very different in the two cases of H and E polarizations.

In the H polarization, corresponding to currents flowing perpendicular to the strike, it is not possible to determine the underground conductivity structure from measurements of the magnetic field alone, but if the electric field E_y is also measured, the apparent resistivity ρ_A , given by the usual magnetotelluric formula, can be calculated. It is found that ρ_A over a surface anomaly of high conductivity is practically constant over the whole anomaly (A, B, C, of Fig. 6), but significantly smaller (in the cases studied) than the true resistivity; i.e. the magnetotelluric formula gives an apparent conductivity for the anomalous region that is actually higher than the true conductivity anywhere in the model structure. Now, if the width of the anomaly were made sufficiently large, the calculated ρ_A would closely approach the true resistivity; note for example that ρ_A at points well away from the anomaly gives the correct resistivity for the surrounding conductor. This shows that the calculated ρ_A depends on the width of the anomaly, and confirms the suggestion made by Price (1964) that the lateral dimensions of the more highly conducting regions would appreciably affect the estimates of conductivity obtained by the magnetotelluric method. It would be of great interest to make further calculations for anomalies of different widths to determine this effect more precisely.

Also, in the H polarization case, there are remarkable effects at the edge of the anomaly. On moving from a point on the surface of the surrounding conductor towards a high conducting surface anomaly, the calculated apparent resistivity ρ_A actually increases (curves A, B, C, Fig. 6), and then suddenly drops to a very low value as the edge is crossed. When the edge of a surface anomaly of low conductivity is approached, the apparent resistivity decreases to very low values (curves C, E, F), and rises suddenly on crossing the edge to values somewhat less than the true resistivity.

These edge effects are due, as we have already noted, to the accumulation of charges on the boundaries between media of different conductivities. The electro-

static field of the surface charges adds to the original electric field in the poor conductor and subtracts from it in the good conductor. The additional *conduction* currents produced in the two media by these electrostatic fields serve to equalize the normal components of current flow in the two media, thereby satisfying the boundary condition that the normal component of total current flow must be continuous. It is, of course, important to distinguish between the (minute) current extracted from the original current to set up the (varying) surface charge on the boundary and the conduction currents produced by the electrostatic field of this surface charge. These are true conduction currents depending on the conductivity of the medium, and are not displacement currents. The electrostatic field of the surface charges on the boundary of the anomaly also accounts for the remarkable behaviour of E_y (Fig. 6), and consequently of ρ_A .

In the case of the E polarization, the results shown in Figs 7, 8 and 9 suggest that considerable information about the conductivity structure may be obtained from the magnetic measurements above. For example, the rapid change of phase of the vertical component (Fig. 9) could reveal the edge of an anomaly and the conductivity change involved.

When E_x is also measured, magnetotelluric methods would give a value of the apparent resistivity ρ_A which accords well with the true resistivity (Fig. 8). The slightly larger value of ρ_A for the surface anomalies (A, B, C) is readily explained by the fact that the conductor below the anomaly has a higher resistivity.

The surface effects for buried anomalies are naturally smaller than those for surface anomalies, but will clearly be sufficiently large in many cases to give some information about the underground structure.

The curves D, E, F in all the diagrams show that it will be less easy to detect and investigate anomalies having a conductivity *less* than that of the surrounding medium.

Acknowledgments

We wish to thank the University of Exeter for permission to use the University Computer upon which the preliminary work was done, and to thank the University of Alberta Computing Center for the use of their computer in running the final programs. One of us (F.W.J.) wishes to thank the National Research Council of Canada for financial assistance in the form of a postdoctorate fellowship during his stay in England.

F. Walter Jones:
Department of Physics,
University of Alberta,
Edmonton, Canada

Albert T. Price:
Department of Mathematics,
University of Exeter,
Exeter

References

- Jones, F. Walter & Price, Albert T., 1969. *IAGA Bulletin* No. 26. Abstract III-106, p. 196.
 Jones, F. Walter & Price, Albert T., 1970. *Geophys. J. R. astr. Soc.*, **20**, 317-334.
 Jones, F. Walter & Price, Albert T., 1971. *Geophysics*, **36** (1), 58-66.
 Price, Albert T., 1964. *J. Geomagn. Geoelect.*, **15**, 241-248.